

Study of Alkylglycerol Containing Shark Liver Oil: A Physico Chemical Support for Biological Effect?

Jean-Claude Debouzy¹, David Crouzier¹, Bertrand Lefebvre² and Vincent Dabouis¹

¹Unité BCM Centre de Recherches du Service Santé des Armées, 24, avenue des maquis du Grésivaudan, BP 87-38 702 La Tronche Cedex, France. ²Unité de Biospectrométrie Centre de Recherches du Service Santé des Armées, 24, avenue des maquis du Grésivaudan, BP 87-38 702 La Tronche Cedex, France.

Abstract: Shark liver oil (SLO), is used in natural medicine as immunity stimulant, cardiovascular protector and anti ageing reagent. These properties were related with the high amounts of alkylglycerols (22%) obtained from Greenland shark liver. After a control of the mean SLO composition by NMR and MS, surface and membrane interactions and antioxidant properties were investigated using NMR, ESR and ST measurements and the in vitro consequences on erythrocytes and cells were studied. An estimation of the composition of this extract was performed. Moreover, SLO was found not haemolytic (A concentration inducing 50% haemolysis, HC₅₀ could not be reached) and superficial tension measurements revealed slight tension active properties. The ³¹P and ²H-NMR and ESR studies of phospholipid dispersions (dimyristoyl phosphatidyl cholin, DMPC) in the presence of SLO showed a significant increase in membrane fluidity at low temperature (below phase transition temperature) predominantly observed at the surface level. The anti oxidant activity was also confirmed, similar as that observed for vitamin E.

Keywords: alkylglycerol, membrane fluidity, ESR, NMR, anti oxidant properties

1. Introduction

Greenland sharks, and especially *somniosus microcephalus* are very robust species well adapted to hard environmental conditions such as deep and cold surroundings. In empiric traditional Scandinavian medicine, meat and oil from Greenland shark have been extensively used for healing of wounds, physical stress tolerance, and also immune stimulation and antitumor properties. These uses continuously faded out during the 19th century until early 20th when specific lipids (up to 50% in shark livers [1]) were identified as alkylglycerols [2] (1-*O*-alkyl-2,3-diacylglycerols and their methoxy derivatives [3]). This led to the first trials of A. Brohult [4] who evidenced increased production of granulocytes and thrombocytes and proposed the use of alkylglycerols to counterbalance the bone marrow depletion after radiotherapy in the therapy of carcinomas of the uterine cervix [5]. Later, alkylglycerols have been found to inhibit the growth and spread of transplanted or chemically induced tumors [6]. Immunological system stimulation was also identified, leading to bacteriostatic properties. It is noteworthy that the same substance, shown to be effective *per os*, exhibited both immunoreactivity stimulating and antitumor activity. Among the different mechanisms proposed, the ability of alkylglycerol to penetrate the cell membranes would stimulate the body's own defense system, mainly the macrophages. Besides, the results found when alkylglycerol was given before radiotherapy would also support the hypothesis of a direct interaction with radio induced free radical production. However, no precision of the mechanism involved was clearly proposed at the molecular level. This led us to investigate the biophysical properties of shark liver oil (SLO), the commercial form, by using both NMR and ESR spectroscopies, and assignment biophysics methods both in synthetic systems (phospholipidic membranes) and in red blood cells.

Experimental

Materials

ALKYROL[®]

ALKYROL[®] oil extract from Greenland shark liver was purchased by NUTRILYS[®] Company (Divonne les bains, France) and used without further purification. As this extract is a natural mixture, the amounts

Correspondence: Jean-Claude Debouzy, Centre de Recherche du Service de Santé des Armées, 24, Avenue des maquis du Grésivaudan, BP 87, 38702 La Tronche Cedex France. Tel: (33) 4 76 63 69 39; Fax: (33) 4 76 63 69 22; Email: jcdebouzy@crssa.net



Copyright in this article, its metadata, and any supplementary data is held by its author or authors. It is published under the Creative Commons Attribution By licence. For further information go to: <http://creativecommons.org/licenses/by/3.0/>.

of SLO are better expressed in this paper in mg rather than in mM concentrations (even if the apparent density was estimated at 0.71).

This product was characterized by NMR (see Fig. 1 for peak assignment) and MS (ES+) analysis. As major MS peaks were found at $m/z = 701$; and also 633; 517; 351 ($m/2z$), and from $^1\text{H-NMR}$ peak integration and ^{13}C direct spectra and DEPT datas, an very coarse estimation of the mean apparent molecular weight $M\#650$ was proposed SLO. The corresponding molar ratios might be considered as only indicative and close to W/W ratios (molecular mass for Dimyristoylphosphatidylcholine, DMPC, is 678).

Chemicals

Dimyristoylphosphatidylcholine (DMPC), egg yolk phosphatidylcholine (EPC), and deuterated solvents were purchased from Sigma (La Verpillère, France) and were used as received. Chain perdeuterated DMPC- d_{54} was from Interchim, Montluçon, France.

Multibilayers (MLV)

DMPC liposomes for ^{31}P experiments were prepared in pure deuterated water by successive

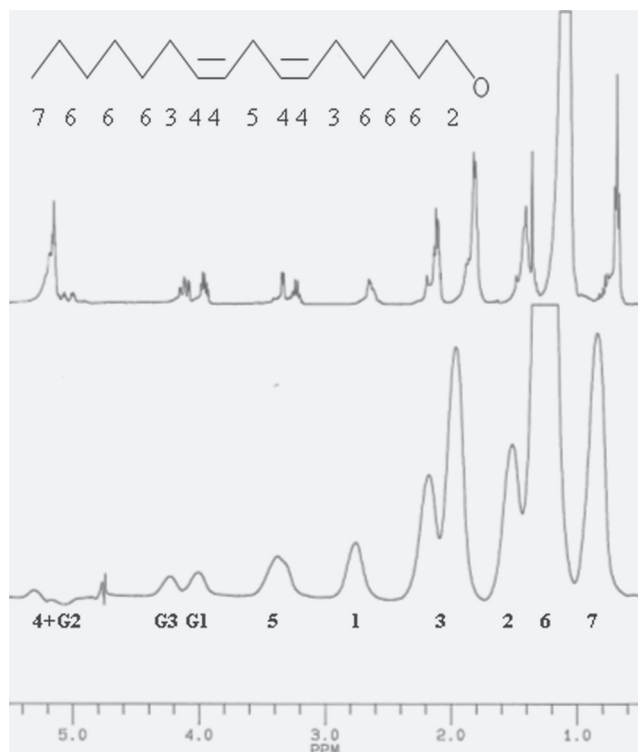


Figure 1. Top: proton nomenclature used for acyl chain labeling; middle: $^1\text{H-NMR}$ spectrum of SLO; 1 mg in CDCl_3 , 298 K; bottom: 1 mg in D_2O , 298 K; Glycerol proton labeling: G1, G3, methylenic groups, G2, methinic group.

freezing and thawing cycles [7] until an homogenous milky sample was obtained. [8] The suspensions were degassed under nitrogen gas then introduced into NMR tubes and sealed. The final lipid concentration was 50 mM (in 500 μL samples), while SLO/DMPC in mixed systems was ranged from 1/50 to 1/25, mg/M. The same procedure was used for multilayers for $^2\text{H-NMR}$ experiments, except that 25% DMPC with perdeuterated chains were used (DMPC- d_{54}) to build the liposomes.

Methods

Haemolytic activity

All procedures were in accordance with the standards for animal care established by our institute and were approved by our animal use ethic committee (decree 87-848 19 October 1987).

Blood from male Sprague-Dawley rats was collected in heparinated tubes and washed twice using isotonic NaCl solution; the hematocrit was then brought to 10%. 1 mL cuves were filled with the SLO solutions to test (0 to 32 μL) in 50 μL of DMSO and with 100 μL of the diluted blood in saline. The samples were stocked for 1 hour at 37 $^\circ\text{C}$, then centrifuged at 2400 rpm, 4 $^\circ\text{C}$ for 10 minutes. Absorption measurements were finally performed on a Shimadzu MCS-2000 absorption spectrometer at 540 nm, as described elsewhere. [1, 9]

The haemolytic activities were expressed in terms of HC_{50} , the concentration giving 50% haemolysis as referenced to i) the total haemolysis induced by triton X-100 addition or on sonicated samples ii) the absence of any haemolysis (0% haemolysis) evaluated on samples where only isotonic NaCl (0.9% W/W) solution was added.

NMR experiments

All NMR experiments were recorded on a Bruker AM-400 spectrometer. $^1\text{H-NMR}$ spectra in D_2O were acquired at 298 K using a presaturation of the water resonance and a spectral width of 10 ppm. The chemical shifts were referenced by setting the water resonance at 4.75 ppm. $^1\text{H-NMR}$ control spectra were recorded using classical 1D and 2D (COSY, TOCSY (Sanders, 1989) experiments at 300 K, 2 mg, in perdeuterated di methyl sulfoxide (DMSO- d_6).

In $^1\text{H-NMR}$ T_1 and T_2 measurements in water preparation (1 mg, D_2O , 298 K) used the inversion recovery method [10] with a 10 ppm line width and a 5sec recycling delay to ensure relaxation.

Partition coefficient (LogP) calculation was realized by using an NMR method derived from the classical Shake-flask method [9]: A first ^1H -NMR spectrum was recorded acquired as previously in water, while using 1 mg SLO in 1 mL D_2O to ensure that the NMR observation area is fully included in the aqueous solution. Then an equal volume (1 mL) of perdeuterated octanol was added, and the sample vortexed and centrifugated to allow phase separation. The octanol phase was then removed. Another spectrum was the acquired and the intensity signal **I** (that of CH_3 at 0.89 ppm) compared to the intensity of SLO in pure water, (**I**₀). Thus, if $\mathbf{R} = \mathbf{I}/\mathbf{I}_0$, i.e. the remaining fraction of SLO in the water,

$\mathbf{P} = (\mathbf{1}-\mathbf{R})/\mathbf{R}$ gives the partition in the sample, and the partition coefficient LogP is obtained by

$$\text{LogP} = \log((\mathbf{1}-\mathbf{R})/\mathbf{R})$$

^{31}P -NMR experiments were performed at 162 MHz. Phosphorus spectra were recorded using a dipolar echo sequence ($\pi/2$ -t- π -t) [11] with a t value of 12 μsec and a broadband two levels proton decoupling $\pi/2$ pulse was 4.8 μs , recycling delay of 5sec. Phosphoric acid (85%) was used as external reference. Uncoupled spectra and partial continuous wave proton low level decoupling (24L) were also used to measure phosphorus-proton coupling constants.

^2H -NMR experiments were performed at 61 MHz. MLV were formed as for ^{31}P experiments whereas in deuterium depleted water. Deuterium spectra were recorded by using a quadrupolar echo sequence ($\pi/2$ -t- $\pi/2$ -t) with a t value of 20 μsec ; $\pi/2$ pulse was 8 μs and recycling delay of 15sec. The free induction decay was shifted by fractions of the dwelling time to ensure that its effective time for the Fourier transform started at the top of the echo.

Surface tension measurements

Measurements were done on a Tensiometer CSC-Du Nouy (CSC N°70535) using the ring method of measurement in 20 ml of water. Pure water from MilliQ (18.2 M Ω .cm) was used as reference (75.8 mN/m at 293 K).

Electron spin resonance (ESR): spin trapping investigation

Anti radical activity was assessed by in vitro spin trapping experiment. Reactive oxygen species were

generated immediately before ESR experiment by a Fenton reaction (FeSO_4 , 0.1 mM and H_2O_2 , 0.1 mM). The formation of short-lived radical species ($\cdot\text{OH}$) was evidenced by addition of Water Soluble α -(4-pyridyl-1-oxide)-N-t-butyl nitron (4-POBN) (Sigma, France) at 150 mM (in DMSO/ H_2O solution 5% V/V) spin trapping agent. Reaction was performed in an Eppendorf tube, 100 μL of FeSO_4 were mixed with 100 μL of 4-POBN spin trap and with 2 μL of Alkyrol[®]. The trigger of reaction was performed by adding 100 μL of H_2O_2 . Reference samples were prepared by replacing Alkyrol[®] by distilled water, Anti radical properties were also compared by replacing Alkyrol[®] by 2 μL of Vit E.

The samples were transferred in 20 μL Pyrex capillary tube, an placed in 3 mm diameter quartz holder.

The spectra were acquired using the continuous wave mode with a ESP 380 (Bruker) ESR spectrometer, operating at a microwaves frequency of 9.71 GHz. The instrumental parameter were: microwave power of 10 mW, modulation frequency at 100 kHz with a modulation amplitude of 0.51 G, receiver gain was 6.30×10^4 and scan range was 70 G with magnetic field centred at 3430 G. Each sample was scanned 3 times at controlled temperature 295 K, with the following acquisition parameters: Time constant 20.48 ms, conversion time 20.48 ms and 5 repetitions. Figure 6 B shows typical ESR spectra of the control groups with the 4-POBN spin trap.

An estimation of free radical promotion was obtained by measuring the amplitude of the central doublet.

ESR spin label study

The fluidity of rat red cell membrane was investigated by ESR spin label experiments. Two spin labels (Sigma France) were used: 5 nitroxide stearate (5 NS) and 16 nitroxide stearate (16 NS). This fatty acids self incorporate the membrane and the nitroxide groups provide information of motional freedom of the label in biological membrane. So the former probes the superficial part of the membrane layer, the latter in its hydrophobic core. [12]

The experiments were performed on rat red cells. The erythrocytes were isolated from fresh blood by centrifugation at 4 °C (10 min, 1000 \times g), then rinsed using saline, recentrifuged,

this procedure being repeated until a clear supernatant was obtained, then brought to 30% packed cell volume. 2 μL of Alkyglycerol solution were added in each 1 mL sample and then labelled with 20 μL of spin label solution (5 ns 10^{-3}M or 16 ns 10^{-3}M). After 30 min incubation at room temperature, sample were transferred by capillarity in 20 μL Pyrex capillary tube. This tube was placed in a 3 mm diameter quartz holder, and insert into the cavity of the ESR spectrometer.

The ESR spectra were recorded at different controlled temperature (288, 293, 298, 303, 310 and 315 K) with the following conditions: microwave power 10.00 mW, modulation frequency 100 kHz, modulation amplitude 2.05 G, receiver gain 6.10^5 conversion time 40.96 ms, time constant 20.48 ms. Sweep range was 160 G with a central field value of 3435 G.

The complete membrane incorporation of the spin labels was ascertained by the absence on the spectra of the extremely resolved ESR lines corresponding to free rotating markers.

5 NS experimentations: The value of outer and inner hyperfine splitting were measured ($2T_{//}$ and $2T_{\perp}$ respectively), on ESR spectra (Fig. 5B), and order parameter S was calculated following the equation: [13]

$$S = 1.723 \times \frac{T_{//} - (T_{\perp} + C)}{T_{//} + 2(T_{\perp} + C)} \text{ With}$$

$$C = 1.4 - 0.053 \times (T_{//} - T_{\perp})$$

The increase of the order parameter value means a decrease of local membrane fluidity.

16 NS experimentations: The changes in freedom motion of 16 NS were analyzed with the calculation of τ_c , the rotational correlation time. τ_c was calculated following the formula: [14]

$$Tc = K \times \Delta W_0 \left(\sqrt{(h_0/h_{-1})} - 1 \right) \text{ With}$$

$$K = 6.5 \times 10^{-10} \text{ s.G}^{-1}$$

In this formula, ΔW_0 is the peak-to-peak line width of the central line; h_0 and h_{-1} are the peak high of the central and high-field lines respectively (Fig. 5C).

The decrease of the rotational correlation time means a decrease of local membrane fluidity.

Mass spectroscopy

The ES-control spectra were acquired in CH_2Cl_2 as solvent with 1% formic acid, using a VG.Quatro II spectrometer from Micromass/Waters, and treated with the Masslink 4.00 V software. The capillary tension was 3.88 kV, and the cone tension and ion energy 88 V and 1.8 V, resolution values were set to 15.2, and the multipliers 1 and 2 set to 650 V.

Investigations and Results

SLO structure evaluation in solution and in water samples

Chloroformic solution

As expected a true solution of SLO was obtained in chloroform (see Fig. 1 top trace) and the control of SLO main composition could be easily obtained from standard 1D and 2D ^1H - ^{13}C - ^{31}P NMR and ES-MS experiments. Especially, no other hydrophobic components such as phospholipids, sterols an squalene were detected and the resonances of glycerol moiety (labeled G1,2,3) and those of the chain (see the nomenclature on the Fig. 1) were clearly identified. As relaxation times were quite homogenous (relaxation times T_1 and T_2 close to 1sec) [15] an estimation of the average length and insaturation of the chains was obtained by building indexes from ^1H -NMR peak integrals as follows:

As shown on Figure 1 the resonance labeled (4) at 5.2 ppm is representative of methynic group; however, since this resonance is completely overlapped by glycerol signal (G2), the unambiguous resonance of methylenic groups (3) nei gighbouring methynic (4) was used. The resonances (5) were representative of polyunsaturation, and terminal methyle peaks (7) of number of chains. For each group, the value of the integral was divided by the corresponding number of protons (3, for methyl, 2 for methylen) to allow a count of the number of groups. Finally, an estimation of the chain length reference, A , was obtained by adding all the weighted resonances 1,2,3,4,5,6 and 7, with subtraction of half the contribution of G1 methylenic group of glycerol (at 4 ppm) to overcome the G2 (CH) contribution at 5.2 ppm.

Within the different samples controlled, no variation exceeded 10% from the following values:

Number of groups per chain; $A/(7) = 19 \pm 2$
 Chain insaturation index: $(3)/A = 10\% \pm 1\%$
 Chain polyinsaturation index: $(5)/A = 4.9\% \pm 0.5\%$, thus indicating a good homogeneity within the different samples used.

MS spectra confirmed this homogeneity by giving exclusively a dominant line at $m/z = 351.9$, another of half the intensity at $m/z = 517$ and four minor components at $m/z = 301-417-467-633$.

Aqueous samples

Depending on chain length and insaturation found, partial apparent solubilization in the water was not excluded. [16] Hence, $^1\text{H-NMR}$ lines were detected on the NMR aqueous sample containing 1 mg SLO (see Fig. 1, bottom trace). However, the linewidths measured (from 30 to 50 Hz) suggested that supramolecular assemblies had been formed, such as micelles or droplets. This led to measure T_1 and T_2 relaxation times. These parameters are closely related to the correlation time τ_c and the volume of the system as classically described following the relations: [17]

$$1/T_1 = R_1 = A \cdot \tau_c \cdot [(1/(1 + \omega^2\tau_c^2)) + 4/(1 + 4\omega^2\tau_c^2)] \quad (1)$$

$$1/T_2 = R_2 = 6A \cdot \tau_c \cdot [4 + 9/(1 + \omega^2\tau_c^2) + 6/(1 + 4\omega^2\tau_c^2)] \quad (2)$$

with $\omega = 400 \text{ MHz}$; $A = \gamma^4 \cdot (h/2\pi)^2 / r^6$; γ the gyromagnetic factor, $(h/2\pi)$ Planck's constant and r the inter spins distance.

Similar relaxation values were found within the molecule ($T_2 = 30 \pm 10 \text{ ms}$, $T_1 = 420 \pm 20 \text{ ms}$) except for terminal methyl groups (resonance 7, $T_2 = 50 \text{ ms}$, $T_1 = 310 \text{ ms}$).

This allowed to calculate the range of correlation time by using the ratio T_1/T_2 as follows:

$$R1/R2 = [(1/(1 + \omega^2\tau_c^2)) + 4/(1 + 4\omega^2\tau_c^2)] / [6[4 + 9/(1 + \omega^2\tau_c^2) + 6/(1 + 4\omega^2\tau_c^2)]] \quad (3)$$

Relation in $\omega^2\tau_c^2$ simplified in a second degree equation giving $\omega\tau_c$ limits (from 1 to 3).

Then, assuming a spherical approximation for the molecular assembly, the Stokes-Einstein relation allows an evaluation of the average apparent volume:

$$\tau_c = \eta V / kT, \text{ soit } V = kT \cdot \tau_c / \eta \quad (4)$$

where $\eta = 0.9 \times 10^{-3} \text{ P}$, (N.s/m^2 at 298 K), $k = 1.38 \times 10^{-23} \text{ J/kg}$, $T = 297$ and V the volume (m^3). Finally, $6 < V < 12 \text{ nm}^3$ corresponding to a 50 \AA diameter. Such assemblies are significantly smaller than small unilamellar vesicles of phospholipids (typically of 10–20 nm radius, with T_1 in the 450–900 ms range and linewidths of 40 to 120 Hz) [18].

From these features, collective properties of SLO could be studied by using these aqueous dispersion in biological medium that organic solutions precluded. By considering the great importance of interfacial systems in biology, such as cell surfaces, complementary physico chemical tests were then performed.

Surface properties

The partition coefficient (LogP) was calculated as described in the method section. The value $\text{LogP} = 1.3$ well confirmed that, even if the solubility in organic solvent—octanol— is more than tenfold that in water, the presence of SLO at the interfacial area is highly probable. As a consequence, possible tensioactive properties had to be tested. The result is shown on Figure 2: starting from 75.8 mN/m (pure water at 293 K) successive additions of SLO resulted in progressive diminution

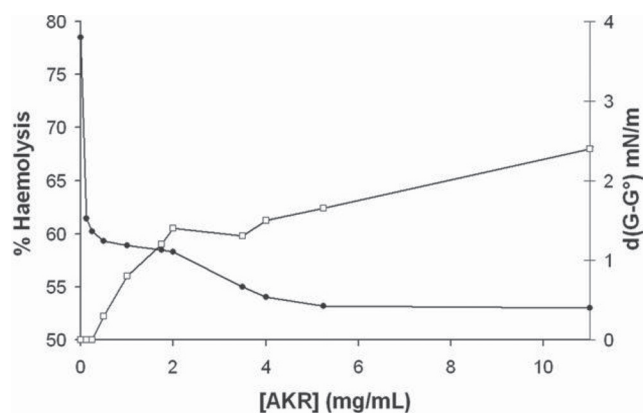


Figure 2. Superficial tension (dG-G° , mN/m), 298 K as a function of SLO concentration (mg/mL) (\bullet), and percentage of haemolysis following the concentration of SLO (\square).

of surface tension down to $ST = 53$ mN/m around 5 mg/mL. Higher amounts of SLO induced no further decrease of ST. Such a limited evolution runs counter any detergent effect or soap-like interactions of SLO, as found for instance for SDS or amphiphilic [19] molecules like cyclodextrins. [20]

However, these negative tensioactive properties suggest interactions with membranes. This point is the topic of the next section.

Membrane structure and dynamics study by ^2H and ^{31}P -NMR

^{31}P and ^2H -NMR spectroscopies of phospholipid dispersions (MLV) were used to observe the structural and dynamics consequences of the presence of SLO at the polar head (^{31}P) and chain (^2H) levels of the membrane.

The polar head group level

As shown Figure 3A (bottom of column), the spectrum of pure DMPC dispersion (MLV) is typical of an axially symmetric powder pattern, with a chemical shift anisotropy of 69 ppm, classical of DMPC bilayers in their liquid crystallin phase around (296 K) phase transition⁷ The chemical shift difference between the lowfield and the highfield edges of the ^{31}P -NMR spectrum is called Chemical Shift Anisotropy (CSA, ppm) and is directly related to the fluidity-reorientation- at the polar head level where the phosphorus nuclei are located. On such spectra a mobile phosphorus group gives a single narrow resonance (several Hz) as detected in true solution or for small structures (micelles), while solide state phosphorus gives extremely broad contributions (more than 100 ppm). Note that membrane fluidity increases (and CSA decreases) with temperature, with a special jump at the transition temperature between gel phase and liquid crystal structure (around 297 K for DMPC). Thus the plot of CSA as a function of temperature provides a good overview of membrane dynamics at the polar head level where phosphorus nuclei are located, while the lineshape allows to identify the overall membrane organisation (bilayer, hexagonal, isotropic phases). Such plots are presented on the bottom traces of the Figure 3: for pure DMPC dispersions and for SLO containing MLV (SLO/DMPC weigh ratios of 1/25 and 2/25 mg/mg) As expected a CSA decrease (around 18–20 ppm) was observed on pure DMPC systems with the transition-related jump around 297 K.

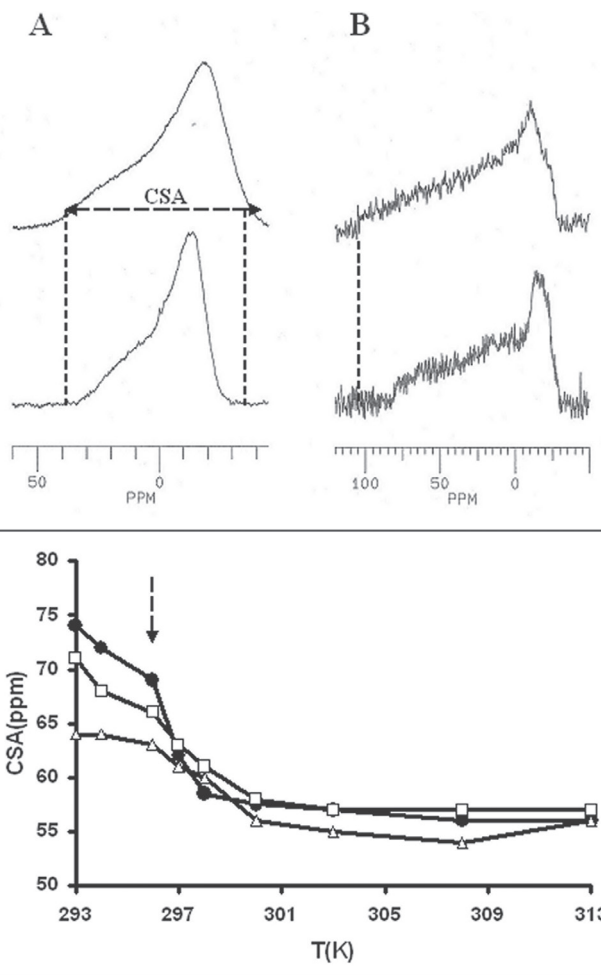


Figure 3. ^{31}P -NMR of DMPC: **Column: A)** typical spectrum of (top) DMPC bilayers (50 mM) close to transition temperature (296 K) (bottom) and in the presence of SLO (SLO/DMPC = 1/25 W/W); **column B)** spectra of ghosts prepared from rat erythrocytes (top), and in the presence of 3 mg SLO (bottom). **Bottom traces:** temperature dependence of the chemical shift anisotropy for pure DMPC (\bullet), and SLO/DMPC systems, 1/25 W/W (\square) and 2/25 W/W (Δ). The arrow indicates the point of the curve corresponding to the top traces.

Such was also the case for the spectra recorded under the same conditions on SLO containing systems at various temperatures. Especially, no isotropic contribution typical of detergent effect was observed. However, a significant reduction in CSA value were measured at low temperature (under transition temperature, see Figure 3A, bottom trace); this increase in local fluidity was not detected at higher temperatures while transition temperature was found unaffected by the presence of SLO (297 K). The presence of structural rearrangements was also supported by this decrease in CSA at low temperature, with a normal transition temperature (297 K) and CSA values close to those of DMPC at higher temperatures.

The acyl chain level

^2H -NMR lineshape

Figure 4A (top) shows the spectrum of DMPC- d_{54} (dimyristoyl phosphatidyl choline with perdeuterated chains) dispersions. This spectrum is typical of phospholipid bilayers in the liquid crystal phase close to transition temperature (296 K) [21]. Such a spectrum appears as a superimposition of symmetrical doublets, each doublet corresponding to a methylenic CD_2 group of the acyl chain. For a given doublet, the splitting ($\Delta\nu_Q$) is directly related to the local order following the relation:

$$\Delta\nu_Q = [A \cdot (3 \cdot \cos^2\theta - 1)] / 2,$$

where A is 170 kHz (for the CD_2 bound in DMPC) and θ the averaged value of the solid angle of reorientation. This splitting can be used in a first approximation as an order parameter. As the acyl chain fluidity decreases from the terminal methyl group (CD_3 , as shown on the expanded part of the spectrum in Fig. 4B) to the methylenic groups close to the polar head of the lipids (the so called "plateau region", from C-2 to C-8 of the chain), the resulting spectrum consists of *i*) an inner doublet with a quadrupolar splitting of 3800 Hz attributed to the CD_3 methyl group, a is found, *ii*) doublets with increasing quadrupolar splittings assigned to successive CD_2 groups from C14 to C9; *iii*) the external edge doublet, attributed to the deuterium of the C2-C8 plateau region where a 29 kHz quadrupolar splitting is measured.

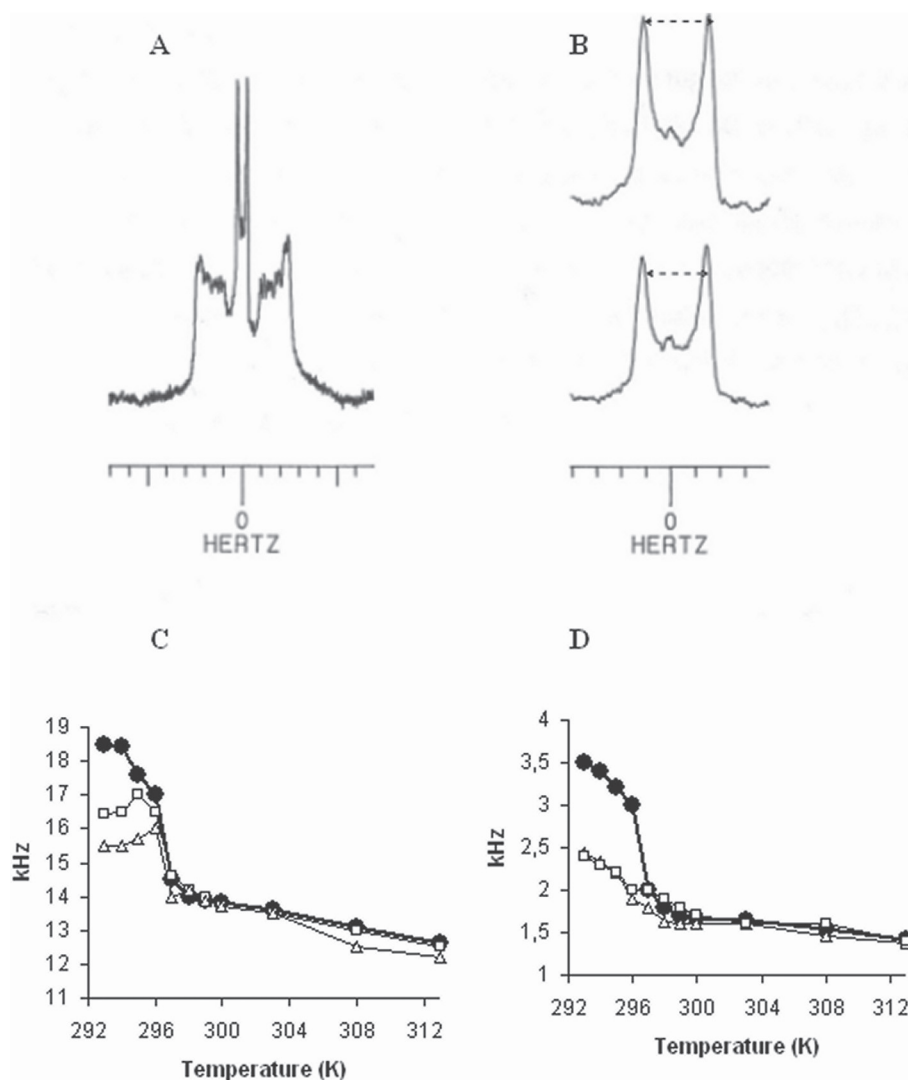


Figure 4. ^2H -NMR spectrum of **A**) pure DMPC- d_{54} dispersions at 296 K (the spectrum is expanded in **B** to show the splitting of CD_3 groups of pure DMPC—*top*— and in the presence of 1 mg SLO—*bottom*—), **Bottom traces** temperature dependence of the half quadrupolar splitting (kHz) for pure DMPC (\bullet), and SLO/DMPC systems, 1/25 W/W (\square) and 2/25 W/W (Δ), for plateau resonances (**C**) and terminal CD_3 group resonances (**D**).

The main spectrum recorded under the same conditions (296 K) in the presence of SLO ($R = 1/25$ and $2/25$ W/W) also shows a dramatic reduction in quadrupolar splittings both at the superficial level (the plateau region) and in the deep part of the membrane (right traces and curves Fig. 4). Besides, no other contribution indicative of isotropic rapid motion was found.

From this part, one can conclude that SLO induces an overall fluidization of synthetic membrane, exclusively present below transition temperature, without inducing any detergent effect and membrane structure and dynamics modification over phase transition. The following step was to test the relevance of these observations in biological systems, i.e. red blood cells, by using macroscopic haemolysis tests and ESR biophysical measurements.

Biological relevance of biophysical results

Haemolytic activity

The haemolysis curve is shown on the Figure 2. By comparison with well identified haemolytic molecules (for instance natural β -cyclodextrin has a 50% haemolytic concentration of 13 mM,) [22] SLO haemolytic activity is found very low, since the maximum haemolysis obtained was 6.6% (21 mg/mL SLO) and 50% haemolysis could not be obtained.

^{31}P -NMR of erythrocyte ghosts

The Figure 3B (top) shows a typical spectrum of red blood cell membranes (100 mg ghosts in D_2O for a total sample volume of 500 μL) recorded at 296 K with the same parameters as DMPC dispersions. Due to cellular organization (cytoskeleton, proteins) the overall membrane structure is significantly more rigid than synthetic systems, according with a CSA (chemical shift anisotropy) of 110 ppm. The addition of 3 mg SLO results in a significant reduction of this value (83 ppm), revealing an increase in collective fluidity without local membrane damages that should have been evidenced by the presence of isotropic line at 0 ppm. However, this effect required at least 2 mg SLO and was not observed for lower amounts.

ESR Spin labeling experiments

Spin label experiments were then realised to investigate the red cells membrane fluidity in different temperature conditions. Two probes were separately used, 5 NS gives information about superficial membrane fluidity, while 16 NS concerned the inner membrane region. The results are shown on Figure 5. An increase of the mobility of the two probes contribution could be observed in SLO groups, related to a global enhancement of the membrane fluidity.

Furthermore, at low temperature (288 K and 293 K), a drop in the order parameter was measured in the SLO group compared to control, that disappeared at the physiological and at the above temperature (up to 315 K). The same observation was done for the rotational correlation time of the 16 NS probe with a decrease of τ in SLO group.

This feature indicated an overall increase of the membrane fluidity of the erythrocytes induced by SLO at the lowest temperature. This effect was not noticeable at physiological temperature.

ESR spin trapping experiments

The Fenton reaction in presence of 4-POBN yields characteristic six-line spectra (Fig. 6B showing 4-POBN results). The spin adduct hyperfine splitting constants were $a_{\text{N}} = 15.73$ G and $a_{\text{H}} = 2.57$ G. According to Finkelstein et al. [23] value: 4-POBN spin trap: $a_{\text{N}} = 15.60$ G and $a_{\text{H}} = 2.55$ G and to Augusto et al. [24] who found $a_{\text{N}} = 15.50$ G and $a_{\text{H}} = 2.50$ G; these hyperfine splitting constants correspond to a α -hydroxyethyl adduct. This is stable adduct results from a reaction between hydroxyl radicals initially generated and the spin trap.

The histogram presented on Figure 6A, shows the free radicals promotion for 3 different concentrations of SLO (8 mg/mL, 0,8 mg/mL and 0,08 mg/mL) versus control and Vitamine E (8 mg/mL). Statistical comparisons were achieved using non-parametric tests (Kruskal-Wallis). Vitamine E is a reference antioxidant molecule able to recombine with free radical. In the presence of Vitamine E and Alkylglycerol in the same concentration, a significant strong decrease in the trace amplitude compared to control was observed (-26% SLO and -28% Vit E). For lower concentrations of SLO (0.8 and 0.08 mg/mL) no significant decrease in spin adduct detection could be shown.

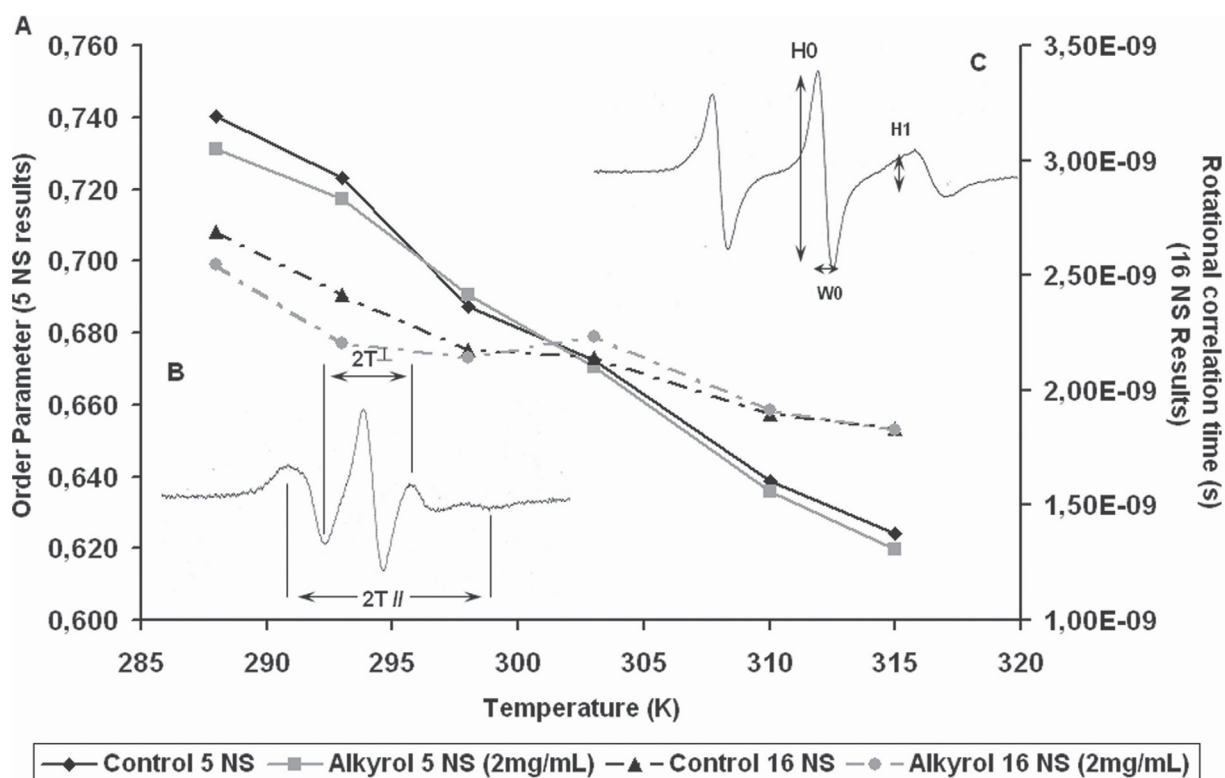


Figure 5. ESR spin labeling experiment. (A) 5 NS and 16 NS results. Left Y axis: temperature dependence of the order parameter (5 NS) for control red cells (black diamond) and Red cell in presence of SLO (grey square). Right Y axis: temperature dependence of the rotational correlation time (16 NS) for control red cells (black triangle) and Red cell in presence of SLO (grey circle). (B) Typical 5 NS spectrum, parameter used for order parameter estimation are inner ($2T_{\perp}$) and outer hyperfine ($2T_{\parallel}$) splitting. (C) Typical 16 NS spectrum, parameter used for rotational correlation time was central peak intensity H_0 , High field peak intensity and the with of the mid-field line W_0 .

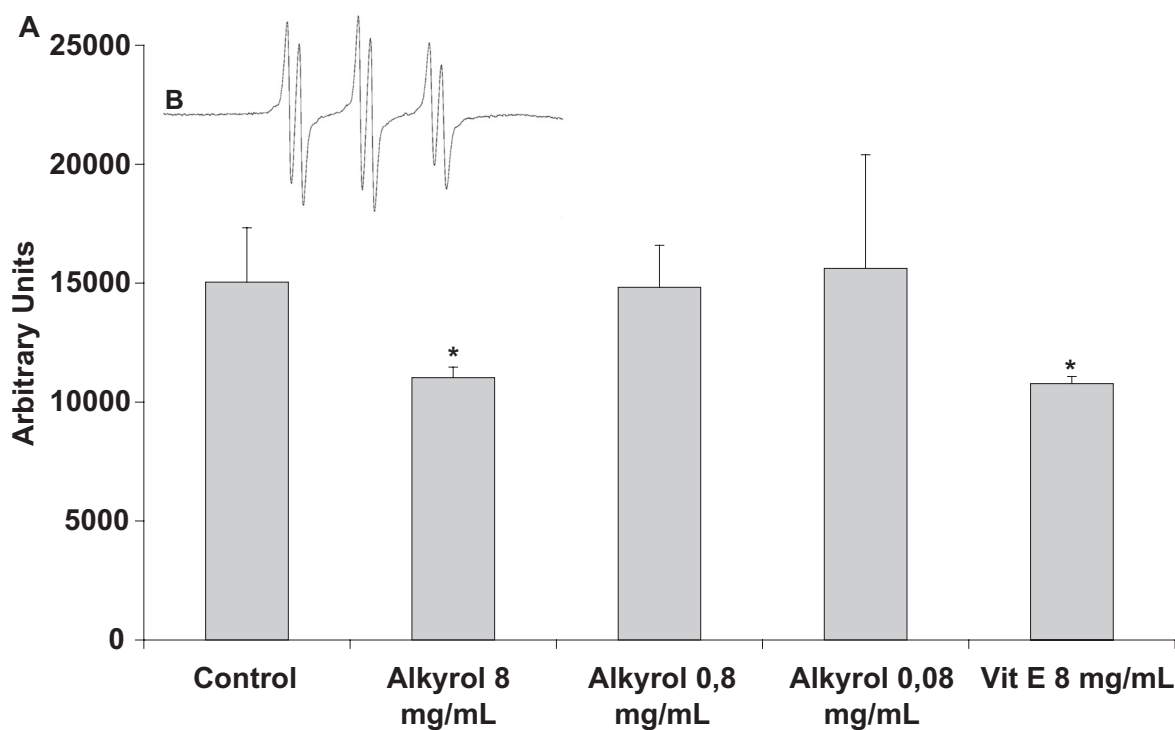


Figure 6. ESR spin trapping experiment. (A) Mean free radical production after exposure using spin trap N-tert-Butyl- α -(4-pyridyl)nitron N'oxide (4-POBN). For each group the value was the average of 3 measurements \pm SD. (B) Typical ESR of N-tert-Butyl- α -(4-pyridyl)nitron N'oxide (4-POBN) radical adducts following Fenton reaction. (*) represents $P < 0.05$.

Discussion

Beside the well established effects of alkylglycerols and polyunsaturated fatty acids on platelet aggregation and inflammatory reactions, the aim of the present work was to investigate physico chemical properties of SLO, especially membrane interactions. This work could be undertaken due to two initial conditions fulfilled:

- the average composition was found homogeneous between numerous samples tested; this was also in agreement with previous analysis showing a composition exclusively made of alkylglycerols and polyunsaturated fatty acids [25] (PUFA);
- due to relatively amphiphilic properties, SLO exhibits a significant solubility in the water, by the way of self-organisation in supramolecular assemblies with an average diameter of 50Å. This point allows the use of SLO in aqueous preparation without requiring to other organic cosolvents (DMSO...) or special preparations (encapsulation...).

The fundamental part of the study, performed on phospholipidic synthetic membranes allowed to identify the fluidization of the membrane, as evoked elsewhere. [26] An intercalation of the oil into the hydrophobic core of the membrane have been observed, affecting the order, packing and overall mobility of the lipid acyl chains. This effect was only observed when the chains are in the gel phase and ordered. This intercalation in the membrane, coupled with possible antioxidant effect should constitute the basis for a reasonably model for its action. However, our results clearly show that a dramatic fluidization is obtained at low temperature, while this effect completely vanishes at temperature (over 296 K). This feature observed both in synthetic systems and in erythrocytes would be of interest in cold environmental conditions if related with the clinical effects expected (a better resistance to intense training...). However, it is worth to note that temperature regulation in sharks is very limited, even at very low temperature. Under this point of view, increased fluidity at low temperature would contribute to maintain cell and tissue functions in extreme environments where sharks live in. By the way of contrast, homeotherms such as humans generally maintain their internal temperature around 37 °C by active metabolic mechanisms such as increasing blood pressure, vasoconstriction and active shivering (from

37 to 34 °C) [27]. Lower temperatures lead to collapses and severe hypothermia to death by ventricular fibrillation. Here the observed effect of SLO at low temperature could appear of limited practical interest. However, in cold environments (e.g. high mountain training, outside work in winter...) cutaneous and subcutaneous temperature are often dramatically lower and SLO properties would play here a physiological role. This is particularly true in some pathologies such as Raynaud's syndrom or microcirculation abnormalities (Malan's syndrome) where both blood cell viscosity and capillary membrane fluidity are involved [28]. Also, cardiac surgery frequently uses extra corporal circulation systems: during operating time, central temperature is set down to 15 °C to protect the brain from the consequences of long lasting hypoxia (20–30min or more). Possible benefits in these circumstances remain to study.

SLO antioxidant properties are also of interest: hence, vitamin E is routinely used as adjuvant agent in radiotherapy, used for its antiradical properties in the prevention of radio induced fibrosis [29]. Another advantage is the apparent extremely low toxicity as tested by insignificant hemolytic activity and complete absence of detergent effect.

Another point of interest is that the amphiphilic properties of SLO are very favorable to overcome biological barrier (cellular membranes, intestinal wall...) by allowing both surface binding and spontaneous cell integration as shown by paramagnetic broadening experiments in cells (not shown). [30] Also, the anti oxidant properties were found similar as those of vitamin E and were related mainly to the general properties of polyunsaturated fatty acids. [31]

Finally, the presence of non specific membrane properties of SLO, associated with its low toxicity is consistent with the great diversity of biological effects evoked in the past, [32] such as anticancer, antioxidant and anti-inflammatory properties. A promising way for future research would be to evaluate the specific applications for work or physical effort in cold environments.

The extreme environmental conditions (pressure and cold) met in all day life of Greenland sharks would also been related with an adaptative Evolutional process leading to optimize biochemical composition of this species. From this point of view, the properties of SLO under high pressure conditions (diving) should also be evaluated.

Aknowledgments

Thanks to J.Morin and T.Lerond for stimulating discussions, and Prof. J.Hàn-peuh-Pluu for manuscript relecture.

Abbreviations

4-POBN: α -(4-pyridyl-1-oxide)-N-t-butyl nitron; 5 NS: 5 nitroxide stearate; 16 NS: 16 nitroxide stearate; CSA: Chemical Shift Anisotropy; EPC: egg yolk phosphatidylcholine; ESR: Electron Spin Resonance; DMPC: dimyristoyl phosphatidyl cholin; HC₅₀: Hemolytic constant 50%; MLV: Multibilayer Vesicle; ES-MS: Electron Spray-Mass spectroscopy; NMR: Nuclear Magnetic Resonance; PAF: Platelet activating factor; SLO: Shark liver oil; ST: Superficial Tension; Vit E: Vitamin E.

References

- [1] Hallgren, B. and Larsson, S. 1962. The glycerol ethers in elasmobranch fish. *Lipid Res.*, 3:31–8.
- [2] Tsujimoto, M. and Toyama, S. 1922. Studies on Unsaponifiable Fractions from Some Fish Liver Oil. *Tokyo Inst. Technol.*, 16:471–510.
- [3] Hallgren, B. and Stallberg, G. 1967. Methoxy-substituted glycerol ethers isolated from greenland shark liver oil. *Acta. Chem. Scand. B.*, 21:1519–29.
- [4] Brohult, A., Brohult, J. and Brohult, S. 1972. Effects of alkylglycerols on the frequency of injuries following radiation therapy. *Experientia*, 57:79–85.
- [5] Brohult, A., Brohult, J. and Brohult, S. 1978. Regression of tumour growth after administration of alkoxyglycerols. *Acta. Obstet. Gynecol. Scand.*, 57(1):79–83.
- [6] Hallgren, B., Niklasson, A., Stallberg, G. and Thorin, H. 1974. On the occurrence of 1-O-(2-methoxyalkyl)glycerols and 1-O-phytanylglycerol in marine animals. *Acta. Chem. Scand. B.*, 28(9):1035–40.
- [7] Dufourc, E.J., Mayer, C., Stohrer, J., Althoff, G. and Kothe, G. 1992. Dynamics of phosphate head group in biomembranes. *Biophys. J.*, 61:42–57.
- [8] Girault, L., Lemaire, P., Boudou, A., Debouzy, J.C. and Dufourc, E.J. 1996. Interaction of inorganic mercury with phospholipid micelles and model membranes. A 31P-NMR study. *Eur. Biophys. J.*, 24:413–21.
- [9] Rappel, C., Galanski, M., Yasemi, A., Habala, L. and Keppler, B.K. 2005. Analysis of anticancer platinum(II) complexes by microemulsion electrokinetic chromatography: separation of diastereoisomers and estimation of octanol-water partition coefficient. *Electrophoresis*, 26(4–5):878–84.
- [10] Sanders, J.K.M., Constable, E.C. and Hunter, B.K. Modern NMR spectroscopy, ed. O.U. Press. 1989, Oxford.
- [11] Mavromoustakos, T., Daliani, I. and Matsoukas, J. 1999. The application of biophysical methods to study drug: membranes interactions, bioactive peptides in drug discovery and design: medical aspects 13–24.
- [12] Debouzy, J.C., Crouzier, D. and Gabelle, A. 2007. Physico chemical properties and membranes interactions of Per (6-Desoxy-6-Halogenated) cyclodextrins. *Annales Pharmacologiques Francaises*, 65:331–41.
- [13] Gaffney, B.J. Practical considerations for the calculation of order parameters for fatty acid or phospholipid spin labels in membranes., in Spin Labelling. Theory and Applications, R.J. Berliner, Editor. 1976, Academic Press: New York London. 567–71.
- [14] Gornicki, A. and Gutsze, A. 2000. In vitro effects of ozone on human erythrocyte membranes: an EPR study. *Acta. Biochim. Pol.*, 47(4):963–71.
- [15] Kaplan, J.I. and Fraenkel, G. NMR of exchanging systems, ed. A. Press. 1980, New York.
- [16] Dennis, E.A. and Plückthun, A. P31-NMR of phospholipids and micelles, in Phosphorus 31P-NMR: Principles and applications, Gorenstein, Editor. 1984, Academic Press: London 423–80.
- [17] Canet, D., Boubel, J.C. and Soulas, E. La RMN, concepts, méthodes et applications, ed. Dunod. 2002, Paris. 235.
- [18] Neumann, J.M., Zachowski, A., Tran-Dinh, S. and Devaux, P.F. 1985. High resolution proton magnetic resonance of sonicated phospholipids. *Eur. Biophys. J.*, 11:219–23.
- [19] Gremy, F. and Leterrier, F. Elements de biophysique, Flammarion, Editor. 1981: Paris 295–304.
- [20] Runhua, L., Jincheng, H., Hanqing, W. and Luinhui, L. 1997. Surface tension measurements and 1H-NMR studies of inclusion complex of beta-cyclodextrin with sodium alkyl sulfonate. *J. of inclusion phenomena and molecular recognition in chemistry*, 28:213–21.
- [21] Douliez, J.P., Léonard, A. and Dufourc, E.J. 1996. Conformational order of DMPC sn-1 versus sn-2 chains and membrane thickness: an approach to molecular protrusion by solid-state 2H-NMR and neutron diffraction. *J. Phys. Chem.*, 100(18):400–57.
- [22] Leray, E., Leroy-Lechat, F., Parrot-Lopez, H. and Duchene, D. 1995. Reduction of the haemolytic effect in biologically recognisable beta-cyclodextrin. *Supramol. Chem.*, 5:149–51.
- [23] Finkelstein, E., Rosen, G.M. and Rauckman, E.J. 1982. Production of hydroxyl radical by decomposition of superoxide spin-trapped adducts. *Mol. Pharmacol.*, 21(2):262–5.
- [24] Augusto, O., Weingrill, C.L., Schreier, S. and Amemiya, H. 1986. Hydroxyl radical formation as a result of the interaction between primaquine and reduced pyridine nucleotides. Catalysis by hemoglobin and microsomes. *Arch. Biochem. Biophys.*, 244:147–55.
- [25] Centre regional de lutte contre le cancer and Montpellier., c.V.-d.A., Métabolisme des lipides pharmacologiques de l'huile de foie de requin. Compte rendu du Comité d'interface de recherché clinique, 1999.
- [26] Singh, G. and Chandran, R.K. 1988. Biochemical and biological effects of fish and fishoils. *Prog. food nutr. Sci.*, 12(4):371–419.
- [27] Meliet, J.L. 2000. Eléments de médecine de la plongée. *Bull Med. Sub. Hyp.*, 10:116.
- [28] Malan, E. Morphogenesis of pezipherical blood vessel-angiodyspasias, ed. C.E. Fond. 1974.
- [29] Delanian, S., Porcher, R., Balla-Mekias, S. and Lefaix, J.L. 2003. Randomized, placebo-controlled trial of combined pentoxifyllin and tocopherol for regression of superficial radiation induced fibrosis. *J. of clinical Oncology*, 21(13):2545–50.
- [30] Debouzy, J.C., Neumann, J.M., Hervé, M., Daveloose, D., Viret, J.J. and Apitz-Castro, R. 1989. Interaction of antiagregant molecule ajoene with membranes. *Eur. Biophys. J.*, 17:211–6.
- [31] Descher, E.E., Lyttle, J.S., Wong, G., Ruperto, J.F. and Newmark, H.L. 1990. The effect of dietary omega-3 fatty acids (fish oil) on azowymethanol induced focal areas of dysplasia and colon tumor incidence. *Cancer*, 66(11):2350–6.
- [32] Pugliese, P.T. and Heineremann, J. Devor disease with shark liver oil, ed. I.C. Inc. 1999, Green Bay WI.